

Optical parametric generation in CdSiP₂

O. Chalus,¹ P. G. Schunemann,² K. T. Zawilski,² J. Biegert,^{1,3,4} and M. Ebrahim-Zadeh^{1,3,*}

¹ICFO-Institut de Ciències Fotoniques, Mediterranean Technology Park, 08860 Castelldefels, Barcelona, Spain

²BAE Systems, Inc., MER15-1813, P.O. Box 868, Nashua, New Hampshire 03061-0868, USA

³Institucio Catalana de Recerca i Estudis Avancats (ICREA), Passeig Lluís Companys 23, Barcelona 08010, Spain

⁴Department of Physics and Astronomy, University of New Mexico, 800 Yale Boulevard,

Albuquerque, New Mexico 87131-0001, USA

*Corresponding author: majid.ebrahim@icfo.es

Received July 28, 2010; revised November 12, 2010; accepted November 14, 2010;

posted November 17, 2010 (Doc. ID 132380); published December 10, 2010

We report efficient generation of picosecond pulses in the near- and mid-IR in the new nonlinear material CdSiP₂ pumped at 1.064 μm by an amplified mode-locked Nd:YVO₄ laser at a 100 kHz repetition rate. By using single-pass optical parametric generation in 8-mm-long crystal cut for type $I(e \rightarrow oo)$ noncritical phase matching, an average idler power of 154 mW at 6.204 μm together with 1.16 W of signal at 1.282 μm has been obtained for 6.1 W of pump at photon conversion efficiencies of 15% and 23%, respectively. Signal pulse durations of 6.36 ps are measured for 9 ps pump pulses. © 2010 Optical Society of America

OCIS codes: 190.4400, 190.4970, 190.7110.

In the absence of widely available solid-state lasers in the mid-IR, optical parametric downconversion has been established as an effective technique for wavelength generation in this spectral range. By exploiting oxide-based birefringent materials, such as LiNbO₃, KTiOAsO₄, and RbTiOAsO₄, or periodically poled crystals, such as periodically poled LiNbO₃ and periodically poled RbTiOAsO₄, spectral regions up to $\sim 5 \mu\text{m}$ can be accessed, but the onset of multiphonon absorption sets a practical upper limit of $\sim 4 \mu\text{m}$ for wavelength generation in such materials. Chalcogenide nonlinear crystals with transparency in the mid-IR, such as CdSe and AgGaSe₂, can provide coherent light at longer wavelengths, but their low bandgap energy precludes pumping near $\sim 1 \mu\text{m}$ due to two-photon absorption, thus requiring long-wavelength laser sources with limited availability near $\sim 2 \mu\text{m}$, or the deployment of cascaded pumping schemes with the associated complexities. It would be imperative to explore more viable alternatives for practical generation of mid-IR radiation beyond $\sim 4 \mu\text{m}$ using direct pumping with Nd-based solid-state lasers near $\sim 1 \mu\text{m}$.

The nonlinear crystal CdSiP₂ (CSP) [1] is a recently discovered optical material that offers unique linear and nonlinear properties for parametric downconversion into the mid-IR [2]. For pumping near 1 μm , CSP has been shown to outperform other mid-IR materials in almost every respect [3]. Importantly, CSP has a bandgap well below 1 μm , which allows pumping at 1.064 μm , and under type $I(e \rightarrow oo)$ parametric generation with noncritical phase matching (NCPM) can provide an idler wavelength near 6.4 μm , a spectral range of great interest for medical applications [4]. In earlier studies, the potential of CSP for the generation of mid-IR radiation using direct pumping at 1.064 μm was demonstrated [5–7]. Using a Q-switched Nd:YAG laser, a CSP optical parametric oscillator (OPO) providing idler pulses with 470 μJ of energy at 6.2 μm at a 10 Hz repetition rate was demonstrated [5]. Soon after, using a pulsed mode-locked picosecond Nd:YAG laser in an oscillator–amplifier format, a synchronously pumped OPO based on CSP, providing idler pulses near 6.4 μm with an energy of 2.8 μJ at 100 MHz, in a train of 2 μs macropulses

at a 25 Hz repetition rate, was reported [6]. More recently, a subnanosecond OPO based on CSP providing idler energy of 24 μJ at 6.125 μm at an average power of 24 mW was demonstrated [7]. Here, we report efficient generation of picosecond pulses in near- and mid-IR in CSP at a repetition rate as high as 100 kHz using single-pass optical parametric generation (OPG) pumped by a mode-locked Nd:YVO₄ laser at 1.064 μm . We demonstrate an average signal power of 1.16 W at 1.282 μm and idler power of 154 mW at 6.204 μm for 6.1 W of pump.

A schematic of the experimental setup is shown in Fig. 1. The pump source is a commercial mode-locked Nd:YVO₄ laser at 1.0642 μm (Lumera Laser GmbH, Hyper 50) in an oscillator–amplifier arrangement, which can deliver up to 40 W of average power at 100 kHz with a pulse energy of 400 μJ . The output beam has a diameter of 5 mm and the pulses have transform-limited durations of 8.7 ps, implying a spectral bandwidth of $\sim 0.2 \text{ nm}$ (assuming Gaussian pulses). The beam quality factor is $M^2 \sim 1.1$, and the output power stability is $<0.5\%$ rms over 13 h. Using a telescope consisting of uncoated fused silica lenses, the pump beam is collimated to a $\sim 500 \mu\text{m}$ diameter before the CSP crystal. The pump power and polarization are controlled by two half-wave plates and a polarizing beam-splitter cube. Pumping is single pass.

The CSP crystal was grown from a stoichiometric melt by the horizontal gradient freeze technique [8]. It was cut at $\theta = 90^\circ$ ($\varphi = 45^\circ$) for type $I(e \rightarrow oo)$ interaction under NCPM with a length of 8 mm and an aperture of 6.75 mm \times 6 mm (along the c axis). The residual loss

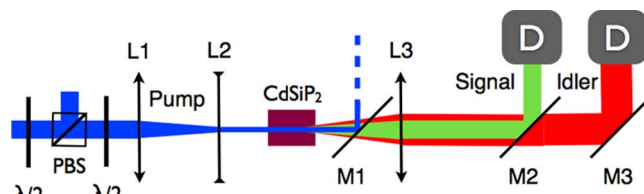


Fig. 1. (Color online) Experimental setup for single-pass CSP optical parametric generator pumped at 1.064 μm . $\lambda/2$, half-wave plate; PBS, polarizing beam splitter; L, lens; M, mirror; D, diagnostics.

of the crystal was measured to be 0.198 cm^{-1} for the pump at $1.064 \mu\text{m}$, 0.114 cm^{-1} for the signal near $1.3 \mu\text{m}$, and 0.014 cm^{-1} for the idler near $6.2 \mu\text{m}$. Both faces were antireflection (AR) coated with an eight-layer coating, providing an average reflectivity per surface of $\sim 0.35\%$ at 1064 nm , $\sim 0.4\%$ at $1.275 \mu\text{m}$, and $\sim 0.5\%$ at $6.2 \mu\text{m}$. The overall single-pass transmission of the AR-coated sample was 83% at $1.064 \mu\text{m}$.

For characterization of OPG output, the pump light after transmission through the crystal was rejected using a 1-mm-thick CaF_2 plane dichroic mirror (M1) with high reflectivity ($R > 99\%$) at $1.064 \mu\text{m}$ and transmitting at the signal and idler ($T = 60\%$ at $1.28 \mu\text{m}$, $T > 90\%$ over $6\text{--}7 \mu\text{m}$). An uncoated CaF_2 lens, L3 ($f = 75 \text{ mm}$), was then used to collimate the generated signal beam, which was separated from the idler using a ZnSe mirror (M2) with high transmission at the idler ($T > 95\%$ over $6\text{--}7 \mu\text{m}$). For the study of the idler, L3 was replaced by another uncoated CaF_2 lens with $f = 50 \text{ mm}$, since the divergence of the idler beam from the OPG was stronger than that of the signal. The idler transmitted through M2 was then finally reflected by a gold mirror (M3) for characterization. In measurements of power and efficiency, all data were corrected for the transmission and reflection losses through the substrates, uncoated surfaces and mirrors.

Using this setup, by gradual increase of pump power, we observed OPG output at an average pump power of 1.1 W at the CSP crystal. This corresponds to a pump pulse energy of $11 \mu\text{J}$ at 100 kHz and pumping intensity of 0.62 GW/cm^2 . By further increasing the pump to 6.1 W , we generated an average signal power of 1.16 W at $1.282 \mu\text{m}$, with corresponding pulse energy of $11.6 \mu\text{J}$. This represents a power conversion efficiency of $\sim 19\%$ and a photon conversion efficiency of $\sim 23\%$ from the pump to the signal. At 6.1 W of pump, we measured an average idler power of 154 mW at $6.204 \mu\text{m}$ with a pulse energy of $1.54 \mu\text{J}$. Therefore, the power efficiency from the pump to the idler was $\sim 2.5\%$, with a photon efficiency of as much as $\sim 15\%$. The lower photon conversion efficiency into the idler is attributed to water absorption in the mid-IR, although additional losses in mirror coatings and substrates cannot be ruled out. Beyond 6.1 W of pump power, we observed the onset of lensing in the CSP

crystal, with the signal and idler beams undergoing strong focusing. To ascertain the origin of this lensing effect, we chopped the pump beam using a mechanical wheel and performed power scaling measurements of OPG output. The results are shown in Fig. 2, where the generated signal pulse energy is plotted against pump pulse energy at the crystal, in the absence of chopping (curve I), and when the pump is chopped at 100 Hz with duty cycles of 50% (curve II) and 5% (curve III). With the pump light unchopped, the signal pulse energy increases linearly for pump pulse energies up to $\sim 40 \mu\text{J}$, beyond which there is evidence of saturation. When increasing the pump pulse energy further, the signal pulse energy rises to $11.6 \mu\text{J}$ for $61 \mu\text{J}$ of pump, at which point we observe focusing of the signal and idler beams. When the pump is chopped, similar linear behavior prevails at low pump energies up to $\sim 40 \mu\text{J}$, but the saturation effect is progressively diminished by reducing the duty cycle. Moreover, under chopped conditions, we no longer observe focusing of the output beams at pump energies above $61 \mu\text{J}$. By further increasing the pump energy, we obtain a signal pulse energy of $14.7 \mu\text{J}$ for $80.9 \mu\text{J}$ of pump at $\sim 18\%$ conversion efficiency with a 50% duty cycle and $17 \mu\text{J}$ for $77.8 \mu\text{J}$ of pump at $\sim 22\%$ conversion efficiency with a 5% duty cycle. However, as is evident, we were not able to completely overcome saturation at higher pump energies even at the highest duty cycle. The results clearly confirm the origin of saturation and lensing as thermal. Given the high repetition rate of the pump laser, saturation in output energy occurs as a result of crystal heating, leading to thermal dephasing at higher average powers. At the same time, focusing of the output beams occurs owing to the strong thermal lens in the crystal at higher pump powers and not higher-order intensity-dependent nonlinear processes, such as the Kerr effect. We attribute the thermal effect mainly to the residual absorption of the crystal at the pump, with some contribution from signal absorption. Since this absorption is not intrinsic, the growth of CSP samples of higher quality

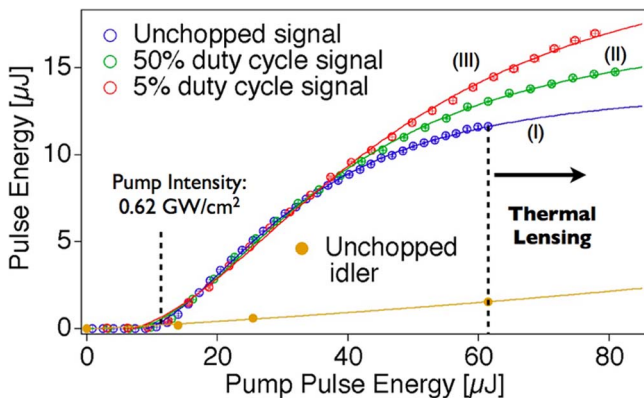


Fig. 2. (Color online) Signal pulse energy versus pump pulse energy. (I) Unchopped pump beam; (II), (III) chopped pump beam. Also shown is the idler pulse energy versus pump pulse energy.

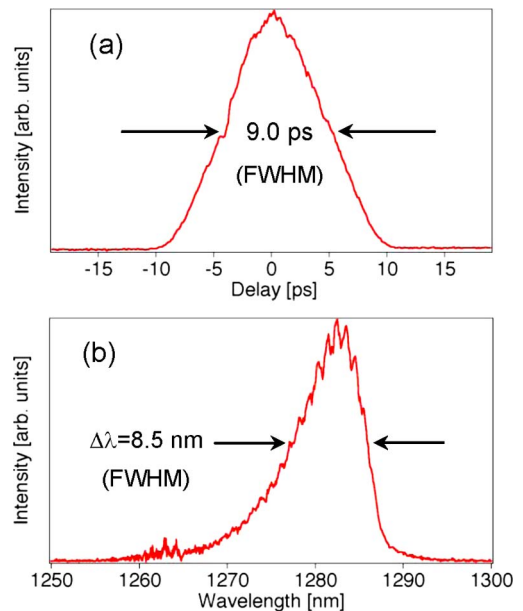


Fig. 3. (Color online) (a) Intensity autocorrelation and (b) spectrum of the signal pulses at $1.282 \mu\text{m}$. Pump power is 2.54 W .

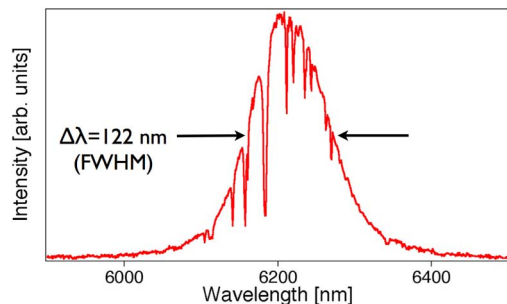


Fig. 4. (Color online) Idler spectrum centered at $6.204 \mu\text{m}$. The sharp features correspond to water absorption lines. Pump power is 2.54 W.

will lead to reductions in saturation and thermal lensing. In addition, with the availability of crystals of larger aperture and length, we expect substantial increases in the signal and idler power to multiwatt and watt levels, respectively, and higher efficiencies, by increasing the pump power to 40 W while minimizing saturation and thermal lensing. In the present setup, the available pump power was limited to 10 W, with ~ 8 W available at the CSP crystal. At the highest pumping intensity of $\sim 4.5 \text{ GW}/\text{cm}^2$ used, we observed no sign of optical damage to the CSP crystal or coatings.

We measured the signal pulse duration using a frequency-resolved optical gating setup based on a $100 \mu\text{m}$ beta-barium borate crystal, where we used the device simply as an autocorrelator. The spectra were acquired using a Fourier transform spectrometer with an InGaAs detector for the signal and a HgCdTe detector for the idler. To avoid detector damage, the pump power was limited to 2.54 W, resulting in 450 mW of signal and 62 mW of idler. Figures 3(a) and 3(b) show the signal autocorrelation and spectrum, respectively. The FWHM of the trace is 9.0 ps, resulting in a signal pulse duration of 6.36 ps (assuming Gaussian pulse shape), and the spectrum is centered at $1.282 \mu\text{m}$ with an FWHM bandwidth of 8.5 nm, resulting in a time-bandwidth product, $\Delta\nu\Delta\tau \sim 9.3$. Using the Sellmeier equations [2], the calculated pump-signal group-velocity mismatch (GVM) is $\sim 231 \text{ fs}/\text{mm}$, resulting in ~ 1.85 ps temporal walk-off

for the 8 mm crystal. The pump-idler GVM is $\sim 843 \text{ fs}/\text{mm}$, with the signal idler having a GVM value of $\sim 612 \text{ fs}/\text{mm}$.

The idler spectrum, shown in Fig. 4, is centered at $6.204 \mu\text{m}$ and has a FWHM bandwidth of 122 nm. The dips in the spectrum correspond to absorption lines of water, as verified by the HITRAN molecular database. The signal and idler peak wavelengths of 1.282 and $6.204 \mu\text{m}$ are in close agreement with the calculated values of 1.286 and $6.180 \mu\text{m}$ for a pump wavelength of $1.0642 \mu\text{m}$ based on the Sellmeier equations for the material [2].

The authors acknowledge support from the European Union (EU) 7th Framework Program, MIRSURG (224042), the Ministry of Science and Innovation, Spain, through Consolider Project (CSD2007-00013), and the European Office of Aerospace Research and Development (EOARD) through grant FA8655-09-1-3017.

References

1. P. G. Schunemann, K. T. Zawilski, T. M. Pollak, D. E. Zelmon, N. C. Ferneliuss, and F. K. Hopkins, in *Advanced Solid-State Photonics*, Conference Program and Technical Digest (Optical Society of America, 2008), postdeadline paper MG6.
2. P. G. Schunemann, K. T. Zawilski, T. M. Pollak, V. Petrov, and D. E. Zelmon, in *Advanced Solid-State Photonics*, Conference Program and Technical Digest (Optical Society of America, 2009), paper TuC6.
3. V. Petrov, F. Noack, I. Tunchev, P. Schunemann, and K. Zawilski, *Proc. SPIE* **7197**, 71970M (2009).
4. G. S. Edwards, R. H. Austin, F. E. Carroll, M. L. Copeland, M. E. Couprie, W. E. Gabella, R. F. Haglund, B. A. Hooper, M. S. Hutson, E. D. Jansen, K. M. Joos, D. P. Kiehart, I. Lindau, J. Miao, H. S. Pratisto, J. H. Shen, Y. Tokutake, A. F. G. van der Meer, and A. Xie, *Rev. Sci. Instrum.* **74**, 3207 (2003).
5. V. Petrov, P. G. Schunemann, K. T. Zawilski, and T. M. Pollak, *Opt. Lett.* **34**, 2399 (2009).
6. A. Peremans, D. Lis, F. Cecchet, P. G. Schunemann, K. T. Zawilski, and V. Petrov, *Opt. Lett.* **34**, 3053 (2009).
7. V. Petrov, G. Marchev, P. G. Schunemann, A. Tyazhev, K. T. Zawilski, and T. M. Pollak, *Opt. Lett.* **35**, 1230 (2010).
8. K. T. Zawilski, P. G. Schunemann, T. M. Pollak, D. E. Zelmon, N. C. Ferneliuss, and F. K. Hopkins, *J. Cryst. Growth* **312**, 1127 (2010).